

# PERFORMANCE EVALUATION OF A COMBINED MULTI-RESOLUTION TEXTURAL CLASSIFICATION OF A SINGLE ERS-1 IMAGE

A. Safia<sup>a,\*</sup>, F. M. Belbachir<sup>b</sup>, T. Iftene<sup>a</sup>

<sup>a</sup> Centre National des Techniques Spatiales, BP: 13, Arzew Oran, Algeria - mas\_safia@yahoo.fr, iftenet@cnts.dz

<sup>b</sup> Dept. (Lab. Signaux, Systèmes et données, USTO, BP: 1505 El Mnaouer, Oran, Algeria mf\_belbachir@yahoo.fr

**KEY WORDS:** Texture-color, radar, classification

## ABSTRACT:

The classification task with only one single monoband radar image, for cost and image availability reasons, is a hard task due to nature of these images. In this paper, we present an attempt for the classification of an ERS-1 radar image for the need of thematic cartography. The drawback of monoband Radar image is surmounted by the integration of the spatial dimension of the image, by using a redundant wavelet transformation. A supervised classification process, which combines both radiometric and textural information's, in a multi-resolution scheme is applied. The results obtained over a single ERS-1 image, which cover a relatively complex area, are satisfactory.

## 1. INTRODUCTION

In a digital image, texture is as an organized spatial phenomenon of pixel values. A texture object is a particular or specific organisation of pixels. Previous methods of analysis for accomplishing texture classification may be roughly divided into three categories: statistical, structural and spectral. These methods have been successful in many fields but they share one common weakness. That is, focus on the coupling between image pixels on a single scale. Among methods allowing multiresolution analysis, the wavelet transform plays an important part in texture analysis. It's well known that SAR (synthetic aperture radar) images have a high textural content. Image classification based on texture features is still a very important aspect in SAR data analysis and segmentation. Various SAR image classifications using textural-based method can be found in literature. In the most cases, the SAR data are used in a multi-date scheme. None of the consulted documentations have been taken into account the classification of a single SAR image, which can be justified by cost or data availability.

This paper is organised as follow. Section 2 presents the area of study and the data used. Sections 3 and 4 present the basic concept of the wavelet transform and its adaptation to the texture analysis task. Sections 5 and 6 describe texture features extraction and classification. Experimental results, discussion and conclusion are given in section 7 and 8.

## 2. DATA ACQUISITION AND STUDY AREA

ERS-1 is a space-based C-band SAR. The radar frequency is 5.3 GHz, with vertical polarization for both transmission and reception. PRI image (precise image) delivered by the ESA (European Space Agency) is a multi-look image. The spatial resolution is 25 m in both azimuth and range. The pixel size is 12.5 m in both azimuth and range. The test site of the present experiment is the Oran region, situated in the west of Algeria (Fig.1). Its location is near 35° 42' N, 00° 38' W. The important features presented in the image were (1) urban, (2) saline, (3)

agricultural zone, (4) naked soil and (5) scrub. Agricultural zone consisted costly of cereal culture and crops. A single PRI image used in our study was acquired on March 21, period on which vegetation is on full growth.

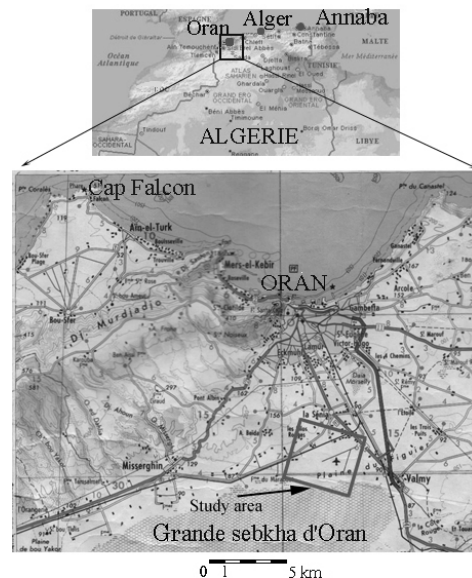


Figure 1. Location of the test site

\* SAFIA Abdelmounaime, Centre National des Techniques Spatiales. BP :Tel : +21341472579. Fax : +21341473665.



Figure 2: The original PRI image

### 3. THE WAVELET TRANSFORM ALGORITHM

Suppose that  $\{V_j, j \in Z\}$  is a multi-resolution analysis in  $L^2(r)$ ,  $\varphi(x)$  is the scaling function of subspace  $V_0$ .  $W_j$  is the orthogonal complement of  $V_j$  with respect to  $V_{j+1}$  i.e.  $V_{j+1} = V_j + W_j$ ,  $\psi(x)$  is wavelet function of subspace  $W_0$ . If a signal  $f(x) \in V_{j+1}$ , then it can be expressed as:

$$f(x) = \sum_n c_n^{j+1} \varphi_{j+1,n} \quad (1)$$

$\varphi_{j+1}$  is the wavelet function relative to detail space.

Since  $V_{j+1} = V_j + W_j$ , then  $f(x)$  can be expressed as:

$$f(x) = \sum_n c_n^j \varphi_{j,n} + \sum_n d_n^j \psi_{j,n} \quad (2)$$

From formula (1) and (2), we have:

$$\sum_n c_n^{j+1} \varphi_{j+1,n} = \sum_n c_n^j \varphi_{j,n} + \sum_n d_n^j \psi_{j,n} \quad (3)$$

Since  $\varphi_{j,k}$  is orthogonal with respect to different  $j$  and  $k$ , if two sides of formula (3) are multiplied by  $\varphi_{j,k}$  and then integrated with respect to  $x$ , we obtain (Mallat, 1989):

$$c_k^j = \sum_n c_n^{j+1} \langle \varphi_{j+1,n}, \varphi_{j,k} \rangle = \frac{1}{\sqrt{2}} \sum_n h_{n-2k} c_n^{j+1} \quad (4)$$

Using the same method, we also have:

$$d_k^j = \frac{1}{\sqrt{2}} \sum_n g_{n-2k} c_n^{j+1} \quad (5)$$

The formulas (4) and (5) are the decomposition formula of signal, where  $c^j$  is an approximation of  $c^{j+1}$ , and  $d^j$  is the detailed part of  $c^{j+1}$ .

If having the decomposed signal  $\{c_n^j, n \in Z\}$  and  $\{d_n^j, n \in Z\}$ , then two sides of formula (3) are multiplied by  $\varphi_{j+1,k}$  and then integrated with respect to  $x$ , we can obtain:

$$\begin{aligned} c_k^{j+1} &= \sum_k c_k^j \langle \varphi_{j,k}, \varphi_{j+1,n} \rangle + \sum_k d_k^j \langle \psi_{j,k}, \varphi_{j+1,n} \rangle \\ &= \frac{1}{\sqrt{2}} \sum_k c_k^j h_{n-2k} + \frac{1}{\sqrt{2}} \sum_k d_k^j g_{n-2k} \\ &= \frac{1}{\sqrt{2}} \left( \sum_k c_k^j \tilde{h}_{2k-n} + \sum_k d_k^j \tilde{g}_{2k-n} \right) \end{aligned} \quad (6)$$

Where  $\tilde{h}_n = h_{-n}$ ,  $\tilde{g}_n = g_{-n}$ . The formula (6) is the reconstruction formula of signal.

The formulas (4), (5) and (6) are called Mallat algorithm (Mallat, 1989).

For two-dimensional signal  $c^{j+1}$  (case of image), the decomposition formulas are:

$$\begin{aligned} c_{m,n}^j &= \frac{1}{2} \sum_{k,l \in Z} c_{k,l}^{j+1} h_{k-2m} h_{l-2n} \\ d_{m,n}^{j1} &= \frac{1}{2} \sum_{k,l \in Z} c_{k,l}^{j+1} h_{k-2m} g_{l-2n} \\ d_{m,n}^{j2} &= \frac{1}{2} \sum_{k,l \in Z} c_{k,l}^{j+1} g_{k-2m} h_{l-2n} \\ d_{m,n}^{j3} &= \frac{1}{2} \sum_{k,l \in Z} c_{k,l}^{j+1} g_{k-2m} g_{l-2n} \end{aligned} \quad (7)$$

The reconstruction formula is:

$$\begin{aligned} c_{m,n}^{j+1} &= \frac{1}{2} \left( \sum_{k,l \in Z} c_{k,l}^j \tilde{h}_{2k-m} \tilde{h}_{2l-n} + \sum_{k,l \in Z} d_{k,l}^{j1} \tilde{h}_{2k-m} \tilde{g}_{2l-n} \right. \\ &\quad \left. + \sum_{k,l \in Z} d_{k,l}^{j2} \tilde{g}_{2k-m} \tilde{h}_{2l-n} + \sum_{k,l \in Z} d_{k,l}^{j3} \tilde{g}_{2k-m} \tilde{g}_{2l-n} \right) \end{aligned} \quad (8)$$

Where  $c^j$  is an approximation of  $c^{j+1}$ ,  $d^{j1}$ ,  $d^{j2}$  and  $d^{j3}$  are the detailed parts of  $c^{j+1}$ . Fig. 3 illustrates the Mallat's algorithm of an image.

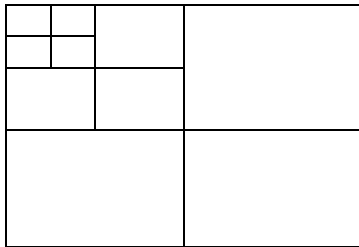


Figure 3. Image Mallat's algorithm decomposition

#### 4. WAVELET TRANSFORM FOR TEXTURE ANALYSIS

Wavelets find various applications such as image compression (Averbuch, 1996 ; Ryan, 1996), noise reduction (Lang, 1996; Gagnon, 1996), data integration [6] and texture analysis (Unser., 1986; Unser, 1995). Wavelets allow discrimination of textures that have similar first order statistics (Unser, 1995). In this paper we use local statistics of the wavelet coefficient in order to characterize texture.

The wavelet transform of a 2-D image can be obtained by performing the filtering consecutively along horizontal and vertical directions with separate filters bank. It yields 4 sub images for one level of decomposition. Every sub image can be sub sampled by a factor of 2, hereby retaining the complete reconstruction possibility. This way, a pyramid of image resolutions is created. We chose not to perform this sub sampling; hence we create a tower of images (Fig. 3.b) instead of the pyramid (Fig. 4.a). The reason is dual: 1) We like to keep the redundant information in the coarse levels to increase the robustness of the transformation to the noise; 2) we maintain a direct correspondence between the pixels across the resolution/ scale levels.

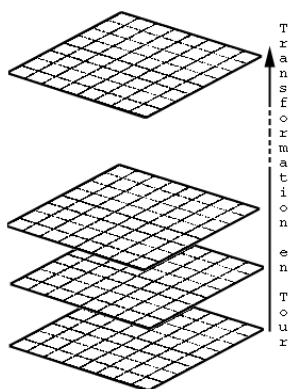


Figure 4. Decomposition diagram

#### 5. TEXTURE FEATURES EXTRACTION

##### 5.1 Which wavelet to choose?

Several studies have tried to answer this important question. There is however no general answer, as some wavelets will be better suited to analyse some particular textures, while other types will be better for others. In this paper, the second order

spline wavelet is used. This wavelet is very sensitive to the local variance, singularity and scene correlation. Thus it is considered appropriate for image texture analysis.

##### 5.2 Wavelet-based texture features

The texture features that are used for texture extraction are simply, local energy and mean measures computed over a window centred on the current spatial position of the approximation images. Two levels decomposition were performed.

$$E = \frac{1}{N} \sum_{\mathfrak{R}} c(i, j)^2 \quad (9)$$

$$M = \frac{1}{N} \sum_{\mathfrak{R}} |c(i, j)| \quad (10)$$

Where N is the total number of wavelet coefficients  $c^j$ , and  $\mathfrak{R}$  is the moving windows calculation. These features have been successfully used for classification and segmentation of textural images. Some authors have attempted to increase classification performance by adding other measures such as the variance. The use of above features is sometimes defended by psycho-visual studies.

#### 6. THE COMBINED CLASSIFICATION BASED ON WAVELET TRANSFORM

Our classification strategy is based on surmounting the drawback of mono band Radar image by the integration of the textural information. The word 'combined' is used to indicate the combination of the textural and radiometric information's, Fig. 5. We perform a decomposition of two levels. Each pixel is characterised by its radiometry and the four textural features. A supervised classification scheme was conducted. It assign each pixel to a given class among the five classes defined on the basis of training parcels chosen with the aid of land-cover map and site visit. The assignment is done according to the Mahalanobis distance minimisation criterion (Schowengerdt, 1983).

The radiometric channel used in addition to the texture information was filtered. But for texture extraction phase, in order to preserve the maximum texture information, we do not perform any speckle reduction for the fact that, the wavelet approximation channels are considered as filtered.

The local windows size is 5x5 for the first level decomposition. Due to the redundant wavelet transform scheme, the estimation of the texture features over the second level approximation image is 11x11.

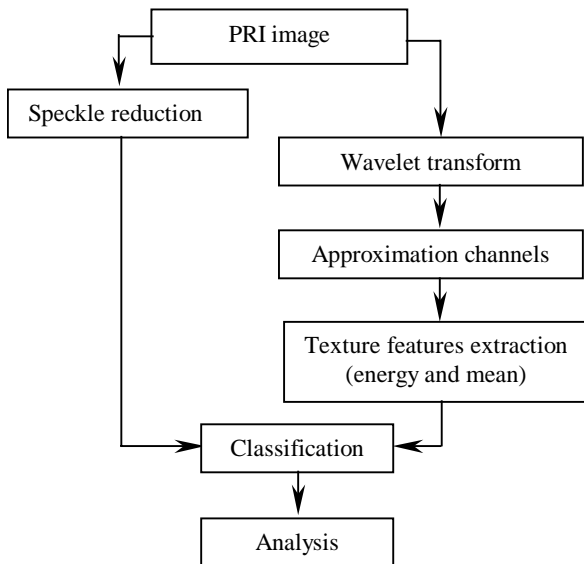


Figure 5. Flow chart of the general methodology

## 7. RESULTS AND DISCUSSION

Classification results in the study area are shown on Fig.6, which represent the land-cover map. Statistics of the classification process are given in the Tab. 1. As can be seen in this table, the classification accuracy is 99% for urban, 100% for saline, 82% for agricultural zone, 81% for naked soil and 51% for scrub.

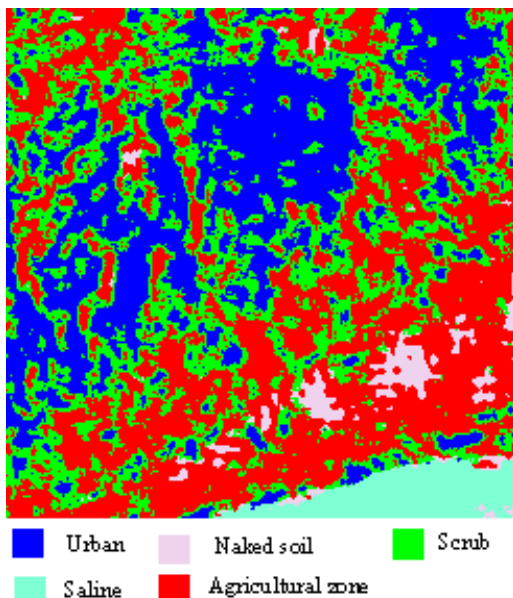


Figure 6. Combined multiresolution classification

	Ground truth pixels				
	1	2	3	4	5
1	99.23 %	0.00 %	0.00 %	0.00 %	17.57 %
2	0.00 %	100 %	0.00 %	0.00 %	0.00 %
3	0.00 %	0.00 %	82.96 %	18.12 %	31.24 %
4	0.00 %	0.00 %	13.50 %	81.88 %	0.00 %
5	0.77 %	0.00 %	3.54 %	0.00 %	51.19 %
Total	100 %	100 %	100 %	100 %	100 %

Global classification accuracy: 80%

Table 1. Confusion matrix

Expected the scrub class, the classification accuracy is acceptable. The principal confusion is between scrub and agricultural zone and urban.

## 8. CONCLUSION

The results obtained for the study area, confirm that the multiresolution combined classification approach can be considered as a good strategy to conduct a classification of a single radar image. But the weak right classification percentage obtained for the scrub class is a good indication of the complexity of the radar image. In further work, we will try to introduce the digital elevation model as an additional canal for more classification efficiency.

## 9. REFERENCES

- Mallat, S., , 1989. A theory for multiresolution signal decomposition: the wavelet representation. IEEE Trans. patt. Ana? Mach. Intell. Processing, vol. 11, no. 7, pp. 674-693.
- Averbuch, D. L. and Israeli, M., 1996. Image Compression Using Wavelet Transform and Multiresolution Decomposition. IEEE Trans. Img. Processing, vol. 5, no. 1, pp. 4-15.
- Ryan, T., Sanders, D., Fisher, H., and Iverson, A., 1996. Image Compression by Texture Modelling. IEEE Trans. Img. Processing, vol. 5, no. 1, p. 26-36.
- Lang, M., Guo, Z., Odegard, J., and Burrus, C., 1995. Non linear Processing of a shift Invariant DWT for Noise-reduction. SPIE Proceeding, Orlando, pp. 640-661.
- Gagnon, L., and Smaili, F. D., 1995. Speckle Noise Reduction of Airborne SAR Images with Symmetric Daubechies Wavelets. SPIE Proceeding, Orlando, pp. 196-207.
- Moon, W., Won, J., Singhroy, V., and Jr., P. L., 1994. ERS-1 and CCRS: C-SAR Data Integration for Look-Direction Bias Correction Using Wavelet Transform. Canadian journal of remote sensing, Vol. 20. no. 3. p.280-286.
- Unser, M., 1986. Local Linear Transforms for Texture Measurements. Signal processing. Vol. 11. p. 61-79.
- Unser, M., 1995. Texture Classification and Segmentation Using Wavelet Frames. IEEE Trans. Img. Processing, vol. 4, no. 11, pp. 1549-1560.
- Schowengerdt, R. A., 1983. Techniques for image Processing and Classification in remote sensing. Academic, San Diego, CA, pp. 181-201.